AIP | The Journal of Chemical Physics

Dynamics of [C3H5N2]6[Bi4Br18] by means of 1H NMR relaxometry and quadrupole relaxation enhancement

W. Masierak, M. Florek-Wojciechowska, I. Oglodek, R. Jakubas, A. F. Privalov, B. Kresse, F. Fujara, and D. Kruk

Citation: The Journal of Chemical Physics **142**, 204503 (2015); doi: 10.1063/1.4919966
View online: http://dx.doi.org/10.1063/1.4919966
View Table of Contents: http://scitation.aip.org/content/aip/journal/jcp/142/20?ver=pdfcov
Published by the AIP Publishing

Dynamics of $[C_3H_5N_2]_6[Bi_4Br_{18}]$ by means of ^1H NMR relaxometry and quadrupole relaxation enhancement

W. Masierak,[1] M. Florek-Wojciechowska,[2] I. Oglodek,[3] R. Jakubas,[4] A. F. Privalov,[5] B. Kresse,[5] F. Fujara,[5] and D. Kruk[6,a)]
[1]*Department of Physics and Material Research, University of Economy, Garbary 2, 85-229 Bydgoszcz, Poland*
[2]*Faculty of Food Sciences, University of Warmia and Mazury in Olsztyn, Oczapowskiego 7, 10719 Olsztyn, Poland*
[3]*Institute of Physics, Jagiellonian University, Łojasiewicza 11, 30-348 Kraków, Poland*
[4]*Faculty of Chemistry, University of Wroclaw, Joliot Curie 14, 50-383 Wroclaw, Poland*
[5]*Institut für Festkörperphysik, TU Darmstadt, Hochschulstr. 6, 64289 Darmstadt, Germany*
[6]*Faculty of Mathematics and Computer Science, University of Warmia and Mazury in Olsztyn, Słoneczna 54, 10710 Olsztyn, Poland*

(Received 11 February 2015; accepted 28 April 2015; published online 29 May 2015)

^1H spin-lattice field cycling relaxation dispersion experiments in the intermediate phase II of the solid $[C_3H_5N_2]_6[Bi_4Br_{18}]$ are presented. Two motional processes have been identified from the ^1H spin-lattice relaxation dispersion profiles and quantitatively described. It has been concluded that these processes are associated with anisotropic reorientations of the imidazolium ring, characterized by correlation times of the order of 10^{-8} s-10^{-9} s and of about 10^{-5} s. Moreover, quadrupole relaxation enhancement (QRE) effects originating from slowly fluctuating ^1H-^{14}N dipolar interactions have been observed. From the positions of the relaxation maxima, the quadrupole coupling parameters for the ^{14}N nuclei in $[C_3H_5N_2]_6[Bi_4Br_{18}]$ have been determined. The ^1H-^{14}N relaxation contribution associated with the slow dynamics has been described in terms of a theory of QRE [Kruk *et al.*, Solid State Nucl. Magn. Reson. **40**, 114 (2011)] based on the stochastic Liouville equation. The shape of the QRE maxima (often referred to as "quadrupole peaks") has been consistently reproduced for the correlation time describing the slow dynamics and the determined quadrupole coupling parameters. © *2015 AIP Publishing LLC.* [http://dx.doi.org/10.1063/1.4919966]

I. INTRODUCTION

Nuclear Magnetic Resonance (NMR) relaxometry is a rich source of information on dynamical and structural properties of condensed matter. Of special importance are field cycling (FC) NMR relaxation experiments which provide spin-lattice relaxation rates over a frequency range covering three orders of magnitude, typically from 10 kHz to $20\cdots40$ MHz (for ^1H). The broad range of frequencies allows to detect motional processes of different time scales by a single experiment. The potential of FC NMR relaxometry is highly appreciated for liquids and soft matter[1–3] but rarely exploited for solids.[4–6] The essential difference between liquid and solid systems is that in the first case, spin interactions are modulated by isotropic dynamics which leads to their zero average, while for solids, the dynamics is typically slow and/or anisotropic which gives rise to dipolar and quadrupolar interactions with non-zero average (they are referred to as residual interactions). In consequence, interpretation of relaxation results for liquids is much easier than for solids. In liquids, the overall spin-lattice relaxation stems from intra-molecular and inter-molecular contributions. In the case of ^1H relaxometry, which is the most common one, the predominant relaxation mechanism is usually the ^1H-^1H dipole-dipole interaction. There are well-known expressions[7–9] describing the relaxation rate as a linear combination of spectral densities taken at ω_H and $2\omega_H$ frequencies, where ω_H denotes the ^1H resonance frequency. The spectral density is defined as the Fourier transform of a time correlation function describing stochastic fluctuations of the dipole-dipole interactions. Intra-molecular dipolar couplings fluctuate due to rotational dynamics of the molecule, while inter-molecular interactions are primarily modulated by translational motion. In consequence, the relaxation studies give access to the rotational correlation time and translational diffusion coefficient.[10,11] If the liquid contains, besides ^1H, other kinds of NMR active nuclei (for instance, ^{19}F, ^{31}P, and ^{14}N), one has to sum up all relevant contributions, then one can apply well-known expressions to describe these relaxation terms.[8,9,12] The established relaxation theory is valid under the condition that the interacting nuclei (spins) exhibit Zeeman energy level structure and that the fluctuations of the interactions responsible for the relaxation are much faster than the relaxation itself. These conditions stem from the validity requirements of the second order perturbation theory applied to derive the relaxation formulae. In solids, the relaxation scenario and, in consequence, the theoretical description are more complex. The residual interactions contribute to the energy level structure of the system (which therefore is not Zeeman anymore). Moreover, slow dynamics puts the system beyond the validity range of the perturbation theory. When one of the participating nuclei exhibits quadrupole interaction

a)Author to whom correspondence should be addressed. Electronic mail: danuta.kruk@matman.uwm.edu.pl. Telephone: +48 89 524 60 11. Fax: +48 89 524 60 89.

(its spin quantum number being equal or larger than 1), for instance, in the case of the ^{1}H-^{14}N dipole-dipole relaxation pathway, one observes a local enhancement of the ^{1}H spin-lattice relaxation rate. This effect is referred to as quadrupole relaxation enhancement (QRE), also often incorrectly called cross-relaxation. A detailed theory of QRE has been given in Ref. 13, and it is outlined in Sec. II. Generally speaking, at magnetic fields at which the ^{1}H energy level splitting (i.e., the frequency ω_H) matches one of the transition frequencies of the nucleus possessing the quadrupole moment (quadrupole nucleus), one observes an enhancement of the ^{1}H spin-lattice relaxation provided the dynamics is slow.[13–16] The positions of the relaxation maxima give a direct access to the quadrupole parameters, while their shape provides information on the time-scale of the fluctuations of the quadrupole interaction, which one can, in most cases, attribute to the reorientational dynamics of the molecule. Moreover, the ^{1}H relaxation dispersion originating from ^{1}H-^{1}H interactions (and interactions with other nuclei of spin 1/2 if present in the compound) is the source of information on the dynamics. As far as the QRE is concerned, the main theoretical difficulties are due to the fact that the slow dynamics combined with strong quadrupole interactions shifts the system outside the validity range of the second order perturbation theory. In consequence, in order to properly describe the QRE effects, one may apply the stochastic Liouville equation (SLE)[13,17–20] or one of the alternative simulation methods in the time domain.[21,22] The treatment presented in Ref. 13 based on the SLE, and therefore valid for arbitrary motional conditions, is a counterpart of the theory of nuclear relaxation in paramagnetic systems in the presence of strong zero field splitting interactions;[19,23] it can also be treated as a generalization of the description presented in Refs. 24 and 25 to an arbitrary spin quantum number. QRE effects are reported in the literature,[26–28] for instance, for proteins[14,29,30] (recently, also in the context of medical applications[28]), but rarely the experimental results are accompanied by theoretical attempts to describe them quantitatively. Vice versa, theoretical papers usually include only a few illustrative experimental examples. Thus, the first goal of the present paper is to apply the theory to a large set of experimental data showing QRE effects. To our knowledge, such attempts of complete and consistent analysis of this phenomenon are not available in the literature so far. For this purpose, we have chosen the compound $[C_5H_5NH]_6[Bi_4Br_{18}]$. This brings us to the second goal of this paper which is the system itself. Halogenoantimonates(III) and halogenobismuthates(III) described by the general formula $R_aM_bX_{(3b+a)}$ (where R denotes an organic cation, M denotes trivalent metal Sb or Bi, and X = Cl, Br, or I) classified as an organic-inorganic hybrid are characterized by an extraordinary diversity of the anionic networks. So far, more than 40 different anionic moieties were found.[31–36] Within the $R_3M_2X_9$ subclass, one can distinguish compounds crystallizing with the chemical composition $R_6M_4X_{18}$ (there are three bridging and three terminal halogens which are characteristic of the $R_3M_2X_9$ stoichiometry). $[C_3H_5N_2]_6[Bi_4Br_{18}]$ (analog based on the imidazole amine) is considered as the most interesting representative of the $R_6M_4X_{18}$ subgroup.[37] $[C_3H_5N_2]_6[Bi_4Br_{18}]$ is built up of a discrete $[M_4X_{18}]^{6-}$ anion which consists of two pairs of edge-sharing octahedrons connected by halogen ligands and three structurally non-equivalent imidazolium cations showing orientational disorder. The structural properties suggest a complex and interesting dynamics of the compound, which we intend to reveal profiting from the potential of ^{1}H NMR relaxometry.

The paper is organized as follows. In Sec. II, the relaxation theory is outlined with special focus on the QRE effects. Section III contains experimental details. In Sec. IV, the data are quantitatively analyzed and the results are discussed. Eventually, Sec. V contains concluding remarks.

II. THEORY OF ^{1}H SPIN-LATTICE RELAXATION AND QRE

As anticipated in Sec. I, a general feature of the ^{1}H spin-lattice relaxation data is the presence of relaxation enhancement peaks superimposed on a relaxation dispersion background. In this section, we shall provide a description of the observed relaxation dispersion features.

The predominant source of ^{1}H relaxation is dipole-dipole interactions. For $[C_3H_5N_2]_6[Bi_4Br_{18}]$, there are several contributions to the ^{1}H spin-lattice relaxation rate, $R_1(\omega_H)$ (ω_H denotes the proton resonance frequency in angular frequency units defined as $\omega_H = \gamma_H B_0$, where γ_H denotes the proton gyromagnetic ratio), resulting from ^{1}H-^{1}H, ^{1}H-^{14}N, ^{1}H-^{209}Bi, and ^{1}H-$^{79(81)}$Br dipole-dipole interactions. Anticipating the forthcoming analysis of the experimental results, one can state that in the frequency range of our experiments, the first two contributions are of primary importance, i.e.,

$$R_1(\omega_H) = R_1^{HH}(\omega_H) + R_1^{HN}(\omega_H), \tag{1}$$

where $R_1^{HH}(\omega_H)$ and $R_1^{HN}(\omega_H)$ denote the relaxation rates originating from ^{1}H-^{1}H and ^{1}H-^{14}N dipolar interactions, respectively. The ^{1}H-^{14}N relaxation contribution, $R_1^{HN}(\omega_H)$, gives rise to the relaxation maxima. This issue will be explained shortly.

If the protons are equivalent (there is no relative chemical shift and they exhibit the same dynamics), the spin-lattice relaxation rate originating from ^{1}H-^{1}H dipolar interactions is given by the well-known equation[7–9]

$$R_1^{HH}(\omega_H) = C_{DD}^{HH}\left[J(\omega_H) + 4J(2\omega_H)\right], \tag{2}$$

where C_{DD}^{HH} is the ^{1}H-^{1}H dipolar relaxation constant, while $J(\omega)$ is a spectral density function being the Fourier transform of a time correlation function characterizing the motional process which leads to time fluctuations of the ^{1}H-^{1}H dipolar interactions. For an exponential correlation function, the spectral density is of Lorentzian shape, $J(\omega) = \frac{\tau_c}{1+(\omega\tau_c)^2}$, where τ_c is a time constant referred to as a correlation time. A closer inspection of the ^{1}H relaxation dispersion data (see Sec. III) indicates at least two motional processes modulating the ^{1}H-^{1}H dipolar couplings. Slow dynamics leads to the strong relaxation dispersion observed at low frequencies, while the higher frequency part of the relaxation dispersion is associated with a faster motion. The expression of Eq. (2) can straightforwardly be generalized to account for several ^{1}H-^{1}H relaxation

contributions,

$$R_1^{HH}(\omega_H) = \sum_i C_{DD,i}^{HH}\left(\frac{\tau_{c,i}}{1+(\omega_H\tau_{c,i})^2} + \frac{4\tau_{c,i}}{1+(2\omega_H\tau_{c,i})^2}\right), \tag{3}$$

where the pairs of parameters $C_{DD,i}^{HH}$ and $\tau_{c,i}$ refer to the individual motional processes.

Before we turn to the ^{1}H-^{14}N relaxation contribution, $R_1^{HN}(\omega_H)$, one should stress that Eqs. (2) and (3) are valid as long as the Redfield condition[8,9,38] is fulfilled, i.e., $\omega_{DD,i}\tau_{c,i} < 1$, where $\omega_{DD,i}$ denotes the coupling constant $C_{DD,i}$ in angular frequency units. As anticipated, the Redfield condition stems from the validity range of the second order perturbation theory applied to derive these equations.

Nuclei of spin quantum number $S \geq 1$ exhibit quadrupole interactions when placed in an electric field gradient. The quadrupole interaction is characterized by a coupling constant a_Q defined as $a_Q = e^2qQ/h$ and an asymmetry parameter, η, where Q is the quadrupole moment of the nucleus and q is the zz component of the electric field gradient tensor. The role of the quadrupole coupling depends on the time scale of its fluctuations. When $\omega_Q\tau_Q \ll 1$ (ω_Q corresponds to a_Q in angular frequency units, while τ_Q is the correlation time characterizing the fluctuations), the quadrupole interaction acts as a source of relaxation of the quadrupole nuclei. Then, the quadrupole relaxation contributes to the modulations of the ^{1}H-^{14}N dipole-dipole interaction (which is the origin of the ^{1}H relaxation). In such a case, the ^{1}H relaxation rate caused by the ^{1}H-^{14}N dipole-dipole coupling is given by the equation[4,13,20]

$$R_1^{HN}(\omega_H) = C_{DD}^{HN}\left[\frac{\tau_{eff}^{(2)}}{1+\left[(\omega_H-\omega_N)\tau_{eff}^{(2)}\right]^2} + \frac{3\tau_{eff}^{(1)}}{1+\left(\omega_H\tau_{eff}^{(1)}\right)^2} + \frac{6\tau_{eff}^{(2)}}{1+\left[(\omega_H+\omega_N)\tau_{eff}^{(2)}\right]^2}\right], \tag{4}$$

with $\omega_N = \gamma_N B_0$ (γ_N denoting the nitrogen gyromagnetic ratio). Equation (4) also applies to other quadrupole nuclei when replacing ω_N by $\omega_S = \gamma_S B_0$ (γ_S denoting the gyromagnetic ratio of the corresponding quadrupole nucleus). The correlation times $\tau_{eff}^{(1)}$ and $\tau_{eff}^{(2)}$ are defined as $\left(\tau_{eff}^{(1)}\right)^{-1} = \tau_c^{-1} + R_{1,Q}$, $\left(\tau_{eff}^{(2)}\right)^{-1} = \tau_c^{-1} + R_{2,Q}$, where $R_{1,Q}$ and $R_{2,Q}$ are the quadrupole (^{14}N in this case) spin-lattice and spin-spin relaxation rates, while τ_c denotes the correlation time describing the "direct" modulations of the ^{1}H-^{14}N dipole–dipole interaction. For rigid molecules (i.e., molecules which do not exhibit internal dynamics), the dipolar as well as quadrupolar interactions are modulated by the same motional process, i.e., $\tau_Q = \tau_c$.

In the opposite motional regime, when $\omega_Q\tau_Q \gg 1$, the quadrupole coupling (which can be in this case considered as time independent) contributes (besides the Zeeman interaction) to the energy level structure of the quadrupole nucleus (of spin S). In consequence, its energy level structure depends on the orientation of the principal axes system (P) of the electric field gradient tensor with respect to the laboratory frame (L) determined by the direction of the external magnetic field, i.e., on the molecular orientation described by the set of Euler angles, Ω_{PL}. Thus, the relaxation rate becomes orientation dependent ($R_1^{HN}(\omega_H,\Omega_{PL})$); it can be obtained from the expression (here, written for the case of ^{14}N)[6,13,19,20]

$$R_1^{HN}(\omega_H,\Omega_{PL}) = C_{DD}^{HN}\left[s_{1,1}(\omega_H,\Omega_{PL}) + 3s_{0,0}(\omega_H,\Omega_{PL}) + 6s_{-1,-1}(\omega_H,\Omega_{PL})\right]. \tag{5}$$

The quantities $s_{m,m}(\omega_H,\Omega_{PL})$ are referred to as generalized spectral densities and can be calculated from the matrix products,[6,13]

$$s_{m,m}(\omega_H,\Omega_{PL}) = \mathrm{Re}\left\{\left[S_m^1\right]^+[M]^{-1}\left[S_m^1\right]\right\}. \tag{6}$$

This formula requires more elaborated explanations. The quantum behavior of the spin S can be described in a basis containing $(2S+1)$ functions defined as $|S,m_S\rangle$, where m_S is the magnetic spin quantum number ranging from $-S$ to S. Thus, for ^{14}N nuclei, the basis consists of 6 functions and it is referred to as Hilbert space. For the purpose of explicitly calculating the spectral densities, $s_{m,m}(\omega_H,\Omega_{PL})$, one has to construct a Liouville space of the dimension $(2S+1)^2$ formed by pairs of the $|S,m_S\rangle$ functions, $\{|S,m'_S\rangle\langle S,m''_S|\}$. The operators S_m^1 are defined as $S_0^1 = S_z$, $S_{\pm1}^1 = \mp S_\pm/\sqrt{2}$. They can be expressed in the basis $\{|S,m'_S\rangle\langle S,m''_S|\}$ as $S_0^1 = \sum_{m_S>0}(|S,m_S\rangle\langle S,m_S| - |S,-m_S\rangle\langle S,-m_S|)$, $S_1^1 = -\sum_{m_S}|S,m_S\rangle\langle S,m_S-1|$, and $S_{-1}^1 = \sum_{m_S}|S,m_S-1\rangle\langle S,m_S|$. The static Hamiltonian of the spin S is a sum of the Zeeman and quadrupole interactions,[8,9,19,20]

$$H_0^{(L)}(S)(\Omega_{PL}) = H_Z(S) + H_Q^{(L)}(S)(\Omega_{PL}) = \omega_S S_z + \frac{1}{2}\sqrt{\frac{3}{2}}\frac{a_Q}{S(2S-1)} \times \sum_{m=-2}^{2}(-1)^m F_{-m}^{2(L)}(\Omega_{PL})\,T_m^2. \tag{7}$$

The superscript (L) explicitly indicates that the Hamiltonian is expressed in the laboratory frame. The tensor operators are defined as $T_0^2(S) = \frac{1}{\sqrt{6}}\left[3S_z^2 - S(S+1)\right]$, $T_{\pm1}^2(S) = \mp\frac{1}{2}[S_z S_\pm + S_\pm S_z]$, and $T_{\pm2}^2(S) = \frac{1}{2}S_\pm S_\pm$, while the spatial components of the quadrupole Hamiltonian are given as $F_{-m}^{2(L)} = \sum_{k=-2}^{2}(-1)^k F_k^{2(P)} D_{k,-m}^2(\Omega_{PL})$, where $F_0^{2(P)} = 1$ and $F_{\pm2}^{2(P)} = \eta/3$. By diagonalizing the matrix representation of the Hamiltonian $H_0^{(L)}(S)(\Omega_{PL})$ in the basis $\{|S,m_S\rangle\}$, one obtains a set of eigenfunctions $\{|\psi_\alpha(\Omega_{PL})\rangle\}$ of the S spin which are linear combinations of the functions $|n\rangle = |S,m_S\rangle$, $|\psi_\alpha(\Omega_{PL})\rangle = \sum_{n=1}^{2S+1} a_{\alpha n}(\Omega_{PL})|n\rangle$. Thus, using the inverse relationship, $|n\rangle = \sum_{\alpha=1}^{2S+1} a_{n\alpha}(\Omega_{PL})|\alpha\rangle$, one can set up the matrix representations $\left[S_m^1\right]$ of the operators S_m^1 in the Liouville basis $\left\{|\psi_\alpha(\Omega_{PL})\rangle\langle\psi_\beta(\Omega_{PL})|\right\}$ ($\left[S_m^1\right]^+$ denotes Hermitian conjugation of $\left[S_m^1\right]$). The matrix $[M]$ is diagonal in the basis $\left\{|\psi_\alpha(\Omega_{PL})\rangle\langle\psi_\beta(\Omega_{PL})|\right\} \equiv |\alpha,\beta\rangle(\Omega_{PL})$ with elements given as[6,13]

$$[M]_{\alpha\beta,\alpha\beta}(\Omega_{PL}) = i\left(\omega_H - \omega_{\beta\alpha}(\Omega_{PL})\right) + \tau_c^{-1}, \tag{8}$$

where $\omega_{\beta\alpha} = \omega_\beta - \omega_\alpha$ denotes the orientation dependent transition frequency between the energy levels ω_β and ω_α (in

angular frequency units) corresponding to the eigenfunctions $|\psi_\beta\rangle$ and $|\psi_\alpha\rangle$, respectively. Eventually, Eq. (6) leads to a linear combination of spectral densities (similarly to Eq. (4)) with orientation dependent contributions and taken at orientation dependent frequencies, $(\omega_H - \omega_{\beta\alpha}(\Omega_{PL}))$. For a very long τ_c, averaging over molecular orientations has to be performed to get the $R_1^{HN}(\omega_H)$ value. At the magnetic field at which $\omega_H = \omega_{\beta\alpha}$, the spectral density $J(\omega_H - \omega_{\beta\alpha})$ reaches a maximum giving rise to a local increase of the $R_1^{HN}(\omega_H)$ relaxation rate referred to as QRE. For $S = 1$, there are three quadrupolar transition frequencies given as (when neglecting the Zeeman contribution to the energy level structure) $\frac{3}{4}a_Q\left(1+\frac{\eta}{3}\right)$, $\frac{3}{4}a_Q\left(1-\frac{\eta}{3}\right)$, and $a_Q\frac{\eta}{2}$ (the last frequency is equal to the difference between the two first ones), thus for ^{14}N, one expects three maxima of $R_1^{HN}(\omega_H)$.

So far, we have discussed the two limiting cases: $\omega_Q\tau_c \ll 1$ (Eq. (4)) and $\omega_Q\tau_c \gg 1$ (Eq. (6)), for which one could apply the perturbation theory considering, in the first case, the quadrupolar interaction as a perturbation stochastically fluctuating in time and therefore leading to the quadrupole relaxation $(R_{1,Q}, R_{2Q})$, while, in the second case, the quadrupolar coupling has been treated as a part of the main (time independent) Hamiltonian determining the energy level structure of the S spin. For the intermediate time scale, the quadrupolar coupling cannot be treated neither as a source of relaxation nor a contribution to the energy level structure. In such a case, the perturbation approach has to be replaced by a full solution of the SLE and the relaxation rate $R_1^{HN}(\omega_H)$ is then given as[13,19,20]

$$R_1^{HN}(\omega_H) = C_{DD}^{HN}\mathrm{Re}\left\{\left[T_1^{1,DD}\right]^+[M]^{-1}\left[T_1^{1,DD}\right]\right\}. \quad (9)$$

This equation is similar to Eq. (6), but the matrices $[T_1^{DD}]$ and $[M]$ have different structures. First of all, the basis is now constructed as an outer product of spin (quantum-mechanical) and dynamical (classical) degrees of freedom, $|O_\alpha\rangle = |\Sigma,\sigma\rangle \otimes |L,K,M\rangle$.[13,19,20,24,25] The vectors $|\Sigma,\sigma\rangle$. represent the spin and they are defined as linear combinations of the $|S,m'_S\rangle\langle S,m''_S|$ vectors,

$$|\Sigma,\sigma\rangle = \sum_{m_S=-S}^{S}(-1)^{S-m_S-\sigma}\sqrt{2\Sigma+1} \times \begin{pmatrix} \delta & \delta & \Sigma \\ m_S+\Sigma & -m_S & -\delta \end{pmatrix}|S,m_S+\sigma\rangle\langle S,m_S|, \quad (10)$$

where Σ ranges from 1 to $(2S+1)$, while () denotes 3j-symbols.[39] The vectors $|L,K,M\rangle$. are associated with the rotational dynamics of the molecule (i.e., rotational modulations of the ^{1}H-^{14}N dipole-dipole axis in this case) and they are defined as[13,19,20,24,25] $|L,K,M\rangle = \frac{\sqrt{2L+1}}{4\pi}D^L_{K,M}(\Omega_{PL})$, where $D^L_{K,M}(\Omega_{PL})$ are Wigner rotation matrices.[39] The basis $\{|O_n\rangle\}$ is, in principle, infinite (due to the classical nature of the rotational dynamics), but the calculations can safely be truncated to $L = 8$. The dipole-dipole interaction between ^{1}H (of spin $I = 1/2$) and the quadrupolar nucleus of spin S, which is the origin of the $R_1^{HN}(\omega_H)$ relaxation, can be described by the Hamiltonian $H_{DD}(I,S) = \sum_{m=-1}^{1}(-1)^m I^1_{-m}T^{1,DD}_m(S)$. The $T_1^{1,DD}(S)$ tensor (relevant to $R_1^{HN}(\omega_H)$) can be expressed as[13,19,20,24,25]

$$T_1^{1,DD}(S) = \sum_{q=-1}^{1}\begin{pmatrix} 2 & 1 & 1 \\ 1-q & q & -1 \end{pmatrix}|1,\sigma\rangle D^2_{0,1-q}(\Omega_{PL}). \quad (11)$$

The matrix $\left[T_1^{1,DD}\right]$ is a representation of $T_1^{1,DD}(S)$ in the basis $\{|O_\alpha\rangle\}$ and it contains only three non-zero elements associated with $|1,-1\rangle\otimes|2,0,2\rangle$, $|1,0\rangle\otimes|2,0,1\rangle$, and $|1,1\rangle\otimes|2,0,0\rangle$;[19,20] the elements are equal to $\begin{pmatrix}1&2&1\\-1&2&-1\end{pmatrix}$, $\begin{pmatrix}1&2&1\\0&1&-1\end{pmatrix}$, and $\begin{pmatrix}1&2&1\\1&0&-1\end{pmatrix}$, respectively. The matrix $[M]$ contains the following elements:

$$\begin{aligned}[M]_{\alpha,\beta} = {} & \frac{1}{4S(2S-1)}a_Q(-1)^{\sigma'}F^{2(L)}_{|K-K'|}\left[(-1)^{\Sigma'+\Sigma}-1\right] \\ & \times\sqrt{(2S+3)(2S+1)(S+1)S(2S-1)(2L'+1)(2L+1)(2\Sigma'+1)(2\Sigma+1)} \\ & \times\begin{pmatrix} L' & 2 & L \\ -K' & K'-K & K\end{pmatrix}\begin{pmatrix} L' & 2 & L \\ -M' & M'-M & M\end{pmatrix}\begin{pmatrix} \Sigma' & 2 & \Sigma \\ -\sigma' & B'-B & \sigma\end{pmatrix}\begin{Bmatrix} \Sigma' & 2 & \Sigma \\ S' & S & S\end{Bmatrix} \\ & +\delta_{LL'}\delta_{KK'}\delta_{MM'}\delta_{\Sigma\Sigma'}\delta_{\sigma\sigma'}\left(\omega_S\sigma+\frac{iL(L+1)}{6\tau_c}\right), \end{aligned} \quad (12)$$

where the states $|\alpha\rangle$ and $|\beta\rangle$ are given as $|\Sigma,\sigma\rangle\otimes|L,K,M\rangle$ and $|\Sigma',\sigma'\rangle\otimes|L',K',M'\rangle$, respectively, while τ_c denotes a correlation time describing stochastic fluctuations of the quadrupole interaction. Equation (9) is valid for arbitrary motional conditions, also including the limits $\omega_Q\tau_c \ll 1$ and $\omega_Q\tau_c \gg 1$. One should stress that the quadrupole relaxation enhancement effects can be only observed for relatively slow dynamics. The correlation time should at least fulfill the condition $\omega_Q\tau_c \cong 1$; for $\omega_Q\tau_c \ll 1$, one does not observe relaxation maxima.

As already anticipated, the relaxation data $R_1(\omega_H)$ contain contributions associated with more than one motional process. Assuming that the motional processes are stochastically uncorrelated and that the imidazolium cations are rigid (i.e., the ^{1}H-^{14}N coupling is modulated by the same motion as the quadrupole interactions of ^{14}N), $R_1(\omega_H)$ is a sum of these

contributions,

$$R_1(\omega_H) = \sum_i R_{1,i}(\omega_H) = \sum_i R_{1,i}^{HH}(\omega_H) + \sum_i R_{1,i}^{HN}(\omega_H)$$
$$= \sum_i \left[C_{DD,i}^{HH} \left(\frac{\tau_{c,i}}{1+(\omega_H \tau_{c,i})^2} + \frac{4\tau_{c,i}}{1+(2\omega_H \tau_{c,i})^2} \right) + C_{DD,i}^{HN} \mathrm{Re} \left\{ \left[T_1^{1,DD} \right]^+ \left[M(\tau_{c,i}, a_{Q,i}, \eta_i) \right]^{-1} \times \left[T_1^{1,DD} \right] \right\} \right], \quad (13)$$

where the matrix $[M]$ depends on the correlation time, $\tau_{c,i}$, and the quadrupole parameters, $a_{Q,i}, \eta_i$, associated with the i-th motional process (the values of a_Q and η can also remain the same for different motional processes, depending on the dynamical scenario and the structure of the compound). We shall use Eq. (13) to analyze, in Sec. III, the $R_1(\omega_H)$ data.

III. EXPERIMENTAL

$[C_3H_5N_2]_6[Bi_4Br_{18}]$ is built up of $[Bi_4Br_{18}]^{6-}$ anions which consist of two pairs of edge-sharing octahedra connected by halogen ligands and orientationally disordered imidazolium cations which occupy three structurally non-equivalent lattice sites. The structure is shown in Fig. 1. The system reveals a rich polymorphism undergoing three phase transitions: I/II at 410 K, II/III at 227 K, and III/IV at 219 K.[37]

^{1}H spin-lattice relaxation dispersion experiments have been performed in the temperature range 236 K–382 K (phase II) using electronic FC relaxometry. The basic idea of this experiment is to measure the spin-lattice relaxation as a function of the magnetic field over a range as wide as possible. This is put into practice by a field cycle in the following way: the sample is initially polarized in an external magnetic field ("polarization field"). After having reached thermal equilibrium, the magnetic field is rapidly switched to a lower field $B_{ev} = \omega_H/\gamma_H$. In this "evolution field", the ^{1}H spin energy levels repopulate (in the simplest case exponentially) with a corresponding spin-lattice relaxation rate $R_1(\omega_H)$ towards the new thermal equilibrium. The corresponding ^{1}H magnetization decay curve is recorded by measuring the FID amplitude in a (high) "detection field", B_{det}, being switched on after a variable evolution time. By carrying out this experiment for many magnetic fields, B_{ev}, the relaxation dispersion profile, $R_1(\omega_H)$, is obtained. For high evolution fields, the field cycle is slightly modified such that, for instance, a zero polarization field is chosen instead of a high one. After having switched to the evolution field, the magnetization will recover from zero up to its new equilibrium, again yielding R_1. The experiments were performed at TU Darmstadt using a home-built electronical FC relaxometer. In our present study, a polarization field corresponding to 30 MHz (^{1}H frequency) and a detection field of 80 MHz were used. The evolution field was varied from about 25 kHz up to 30 MHz. Even if our relaxometer allows for much smaller evolution fields,[41] we restricted our work to the mentioned lower frequency edge because of a residual dipolar field giving rise to a ^{1}H linewidth of slightly above 10 kHz and our desire to stay above the local field. The current source (a Siemens gradient pulse amplifier) allows for a switching time between the diverse fields (polarization field/evolution field and evolution field/detection field) of 1 ms. It then takes another 1 to 4 ms, depending on the actual tuning and regulation parameters, for the evolution field to become stable. This delay determines the shortest accessible spin-lattice relaxation time of about 1 ms. For the present experiments, the FC relaxometer was equipped with an evaporation cryostat covering the mentioned temperature range. For more technical details of this involved setup, we refer to our recent review paper.[40]

The obtained relaxation data are shown in Fig. 2. Several observations can be made already at this stage. The first one is that the relaxation rates show three prominent maxima at

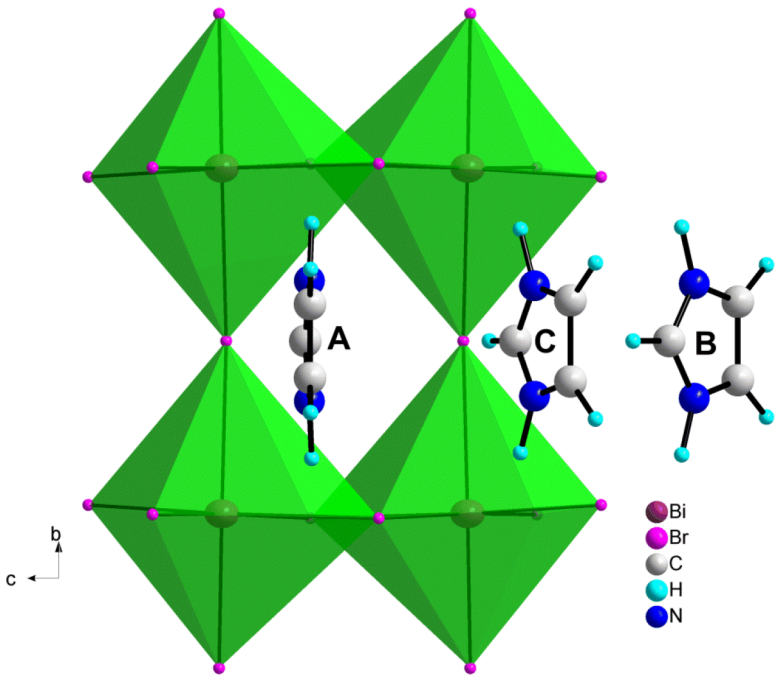

FIG. 1. Scheme of the independent part of the unit cell seen from a view point of the a-axis; A, B, and C denote three structurally non-equivalent imidazolium cations showing orientational disorder (see text).

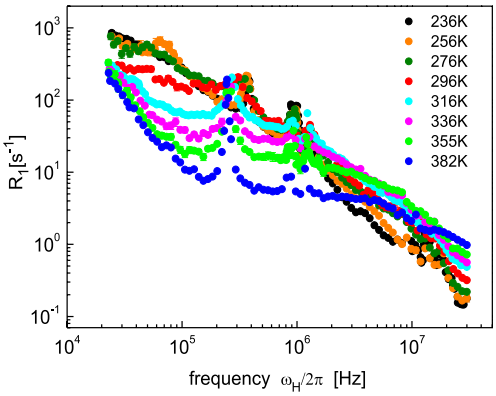

FIG. 2. ^{1}H spin-lattice relaxation rates, R_1, versus frequency for $[C_3H_5N_2]_6[Bi_4Br_{18}]$.

frequencies below 2 MHz. Inspection of these resonances reveals that the lowest resonance frequency corresponds to the difference between the two higher ones, as explained in Sec. II for spin $S = 1$. Next, the relaxation rates at low frequencies increase with decreasing temperature and the low frequency slopes of the relaxation dispersion profiles decrease with decreasing temperature. Keeping this in mind, we begin a quantitative analysis of the relaxation data.

IV. ANALYSIS AND DISCUSSION

We begin the analysis with the highest temperature, 382 K. The relaxation dispersion can be interpreted in terms of two motional processes described by correlation times, $\tau_{c,1}$ and $\tau_{c,2}$, where $\tau_{c,2}$ is associated with the faster dynamics. According to Eq. (13), there are four contributions to the overall relaxation: $R_1 = R^{HH}_{1,1} + R^{HN}_{1,1} + R^{HH}_{1,2} + R^{HN}_{1,2}$. Fig. 3(a) shows the overall fit decomposed into three contributions: $R^{HH}_{1,1}$, $R^{HN}_{1,1}$, and $R^{HH}_{1,2}$. The fitting strategy was as follows. In the first step, the "background" relaxation dispersion profile (neglecting the QRE peaks) has been fitted in terms of two contributions: $(R^{HH}_{1,1} + R^{HH}_{1,2})$, this has led to four parameters: $\tau_{c,1} = 1.2 \times 10^{-5}$ s, $C^{HH}_{DD,1} = 2.0 \times 10^7$ Hz^2 $\tau_{c,2} = 6.1 \times 10^{-9}$ s, and $C^{HH}_{DD,2} = 1.6 \times 10^8$ Hz^2. Inspecting the $R^{HH}_{1,1}$ and $R^{HH}_{1,2}$ relaxation contributions reveals that the relaxation associated with the slower dynamics dominates at lower frequencies, while at higher frequencies, relaxation caused by the fast dynamics has the dominant contribution.

As explained (Eq. (13)), there are also ^{1}H-^{14}N relaxation channels. The $R^{HN}_{1,1}$ relaxation (associated with the slower dynamics) is responsible for the presence of the relaxation maxima. The quadrupolar parameters can be determined from the position of the two maxima at high frequencies $\frac{3}{4}a_Q\left(1+\frac{\eta}{3}\right)$ and $\frac{3}{4}a_Q\left(1-\frac{\eta}{3}\right)$ and confirmed by the position of the low frequency maximum $a_Q\frac{\eta}{2}$; the parameters are $a_Q = 1.32$ MHz, $\eta = 0.37$, $\tau_{c,1} = 1.2 \times 10^{-5}$ s (the slower motional process), and an effective ^{1}H-^{14}N inter-spin distance, $r = 2.4$ Å. The $R^{HN}_{1,1}$ contribution is given by the dashed line in Fig. 3(a). The correlation time, $\tau_{c,2}$, is too short to cause a relaxation enhancement for the $R^{HN}_{1,2}$ contribution. The $R^{HH}_{1,2}$ and $R^{HN}_{1,2}$ relaxation profiles can hardly be separated. Thus, the relaxation process denoted as $R_{1,2}$ (violet solid line) is, in fact, a sum of the two contributions: $R_{1,2} = R^{HH}_{1,2} + R^{HN}_{1,2}$. A sum of all contributions, $R^{HH}_{1,1} + R^{HN}_{1,1} + R_{1,2}$, reproduces the experimental relaxation data (brown line in Fig. 3(a)).

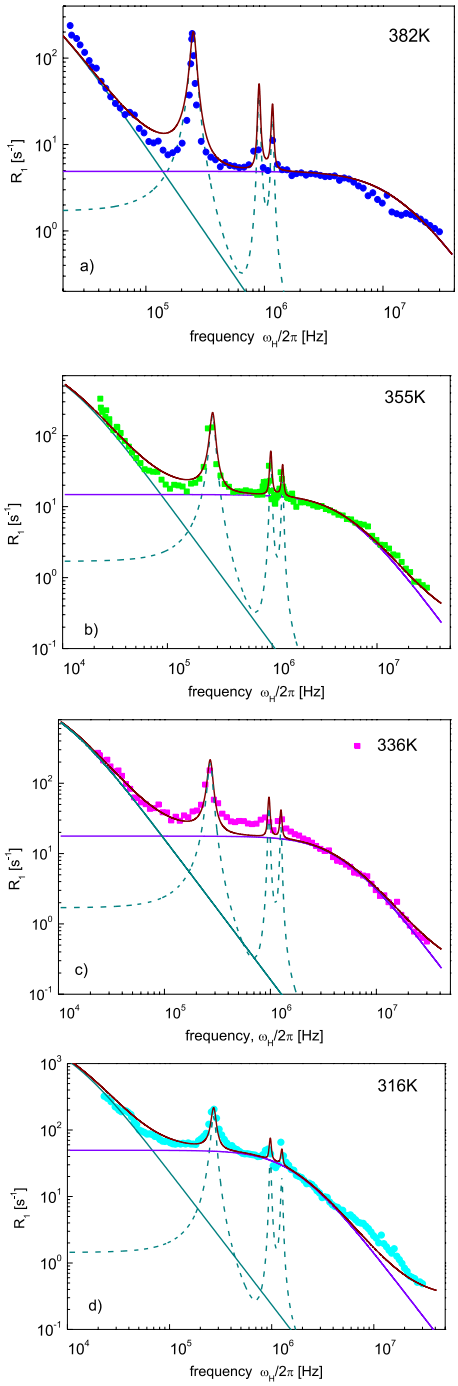

FIG. 3. ^{1}H spin-lattice relaxation rates, R_1, versus frequency for $[C_3H_5N_2]_6[Bi_4Br_{18}]$ at (a) 382 K, (b) 355 K, (c) 336 K, and (d) 316 K. Solid blue line—$R^{HH}_{1,1}$ contribution, dashed blue line—$R^{HN}_{1,1}$ contribution, violet line—$R_{1,2} = R^{HH}_{1,2} + R^{HN}_{1,2}$ term, and brown line—the total fit: $R_1 = R^{HH}_{1,1} + R^{HN}_{1,1} + R_{1,2} + C$.

An analogous analysis has been performed for a lower temperature, 355 K; the results are shown in Fig. 3(b). The R_1 data for 355 K have been reproduced for the same correlation time characterizing the slower motional process, $\tau_{c,1} = 1.2 \times 10^{-5}$ s as the data for 382 K, but a larger dipolar constant is needed, $C^{HH}_{DD,1} = 2.3 \times 10^7$ Hz^2. The correlation time associated with the faster motional processes, $\tau_{c,2}$,

becomes longer as expected with decreasing temperature; the dipolar relaxation constant, $C_{DD,2}^{HH}$, remains unchanged (Table I). The quadrupolar coupling constant, a_Q, now gets somewhat larger, $a_Q = 1.4$ MHz, which is reflected by the positions of the quadrupolar maxima which are now somewhat shifted toward higher frequencies; the asymmetry parameter, η, as well as the inter-spin (^{1}H-^{14}N) distance, r, remains unchanged. Table I contains an additional parameter, C, which denotes a small frequency independent contribution to the overall relaxation originating from other relaxation pathways, like ^{1}H-^{83}Bi or ^{1}H-^{35}Br dipolar interactions.

Before we continue the analysis for lower temperatures, it is worth to inquire how the $R_{1,1}^{HH}$ relaxation rates change with temperature at low frequencies, i.e., in the range in which the slow process dominates. Generally speaking, the relaxation rate decreases with increasing temperature. The maximum of a relaxation rate corresponds to the condition $\omega_H\tau_c \approx 1$ (τ_c denoting a correlation time). For $\omega_H\tau_c < 1$, the relaxation rate increases with decreasing temperature, while for $\omega_H\tau_c > 1$, it decreases. As far as the fast process is concerned, $\omega_H\tau_{c,2} < 1$ holds, which implies that this relaxation contribution increases with decreasing temperature. However, for the slower process, one gets $\omega_H\tau_{c,1} > 1$ already at $\omega_H/2\pi \cong 1 \times 10^4$ Hz, leading to a decrease of this contribution with decreasing temperature, while experimentally at low frequencies, an increase of the relaxation rate with decreasing temperature is observed. This effect cannot be compensated by the faster process (which leads to a relaxation contribution increasing with decreasing temperature) as in the low frequency range, the contribution to the overall relaxation associated with the slow dynamics dominates. This might suggest that the correlation time $\tau_{c,1}$ is much shorter than the estimated value of 1.2×10^{-5} s. However, even a correlation time of the order of 10^{-6} s would not lead to the experimentally observed increase of the relaxation rate R_1 with decreasing temperature still present at frequencies around 100 kHz. Thus, to reproduce the experimentally observed tendency, one should assume an even shorter correlation time, but then one does not observe the quadrupolar relaxation enhancement because of too fast dynamics. Actually, already for $\tau_{c,1} = 10^{-6}$ s, the quadrupolar relaxation maxima would be much broader than those observed experimentally. This leads us to the conclusion that the increase of the relaxation rate R_1 with decreasing temperature can only be explained by a corresponding increase of the dipolar relaxation constant $C_{DD,1}^{HH}$.

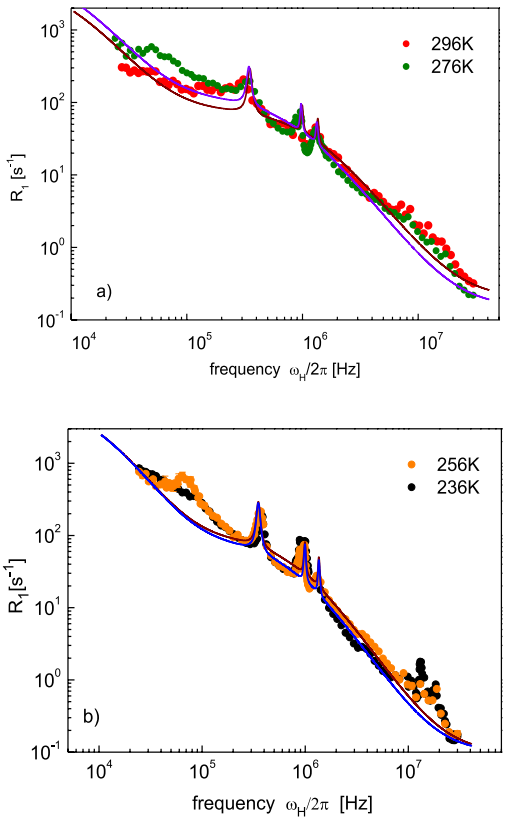

FIG. 4. ^{1}H spin-lattice relaxation rates, R_1, versus frequency for $[C_3H_5N_2]_6[Bi_4Br_{18}]$ at (a) 296 K and 276 K and (b) 256 K and 236 K. Brown lines—the corresponding fits for 296 K and 256 K and blue lines—fits for 276 K and 236 K: $R_1 = R_{1,1}^{HH} + R_{1,1}^{HN} + R_{1,2} + C$.

With this conclusion, we turn to the ^{1}H spin-lattice relaxation data at 336 K and 316 K, which are shown in Figs. 3(c) and 3(d), respectively. The obtained parameters are collected in Table I. As anticipated, to reproduce the low frequency part of the relaxation dispersion profile, one has to assume a larger contribution of the $R_{1,1}^{HH}$ term which can be achieved by gradually increasing the relaxation constant $C_{DD,1}^{HH}$, while the correlation time $\tau_{c,1}$ essentially remains unchanged.

The analysis has been continued for lower temperatures down to 236 K. The results are shown in Figs. 4(a) and 4(b) (here, we do not show the decomposition into the individual relaxation contributions anymore). Actually, the results for the low temperatures, 276 K, 256 K, and 236 K differ only

TABLE I. Parameters obtained from theoretical analysis of the ^{1}H spin-lattice relaxation dispersion data for $[C_3H_5N_2]_6[Bi_4Br_{18}]$. The parameter C denotes a constant which has been added to the theoretical curves to better reproduce the R_1 values at the highest frequencies (see violet lines in Fig. 3); the effective ^{1}H-^{14}N distance yields $r = 2.4$ Å.

T (K)	$C_{DD,1}^{HH}$ (Hz^2)	$\tau_{c,1}$ (s)	$C_{DD,2}^{HH}$ (Hz^2)	$\tau_{c,2}$ (s)	C (Hz)	a_Q (MHz)	η
382	2.0×10^7	1.2×10^{-5}	1.6×10^8	6.1×10^{-9}	0.0	1.32	0.37
355	2.3×10^7	1.2×10^{-5}	1.6×10^8	1.8×10^{-8}	0.2	1.4	0.37
336	3.3×10^7	1.2×10^{-5}	1.6×10^8	2.2×10^{-8}	0.2	1.4	0.37
316	4.8×10^7	1.2×10^{-5}	1.6×10^8	6.15×10^{-8}	0.2	1.4	0.37
296	7.7×10^7	1.2×10^{-5}	1.6×10^8	9.1×10^{-8}	0.2	1.43	0.43
276	1.1×10^8	1.2×10^{-5}	1.6×10^8	1.3×10^{-7}	0.15	1.47	0.43
256	1.1×10^8	1.2×10^{-5}	1.2×10^8	1.35×10^{-7}	0.15	1.47	0.43
236	1.1×10^8	1.2×10^{-5}	9.7×10^7	1.45×10^{-7}	0.15	1.47	0.43

slightly in the range of higher frequencies. The trend has been kept—i.e., all data can be satisfactorily interpreted by increasing (with decreasing temperature) the dipole-dipole coupling constant, $C_{DD,1}^{HH}$, and keeping the correlation time $\tau_{c,1}$ essentially unchanged. Nevertheless, to reproduce the rather small differences at higher frequencies, one has to reduce the dipole-dipole coupling constant, $C_{DD,2}^{HH}$, at 256 K and 236 K. The somewhat shifted positions of the relaxation maxima show that the quadrupole parameters slightly change with temperature. The obtained values are collected in Table I.

Summarizing, applying ^{1}H FC NMR relaxometry, two motional processes have been identified in $[C_3H_5N_2]_6[Bi_4Br_{18}]$ in the temperature range 236 K–382 K (phase II) of this compound. The slower motional process is characterized by a correlation time $\tau_{c,1} = 1.2 \times 10^{-5}$ s and it is very weakly temperature dependent (the correlation time has been kept constant in the whole temperature range). The corresponding dipolar relaxation constant $C_{DD,1}^{HH}$ varies in this temperature range by about factor 5 (from $C_{DD,1}^{HH} \cong 2 \times 10^7$ Hz^2 at 382 K to $C_{DD,1}^{HH} \cong 1 \times 10^8$ Hz^2 at 276 K and below). The faster motional process is characterized by a correlation time $\tau_{c,2}$ ranging from about $\tau_{c,2} \cong 6 \times 10^{-9}$ s at 382 K to about $\tau_{c,2} \cong 1.5 \times 10^{-7}$ s at 236 K. The activation energy of this process in the temperature range 296 K–382 K can be estimated as about 13 kJ/mol; for lower temperatures, the correlation time becomes only weakly dependent on temperature. The corresponding dipolar relaxation constant is $C_{DD,2}^{HH} = 1.6 \times 10^8$ Hz^2, except of the lowest temperatures, 256 K and 236 K, for which it becomes somewhat smaller.

As far as the faster dynamics is concerned, one may think of small-angle oscillations (librations), while the mechanism of the slower dynamical process can be a highly anisotropic rotation or/and large-angle rotational jumps. We cannot identify the specific motional processes, but we consider the following scenario. The observed processes can be parts of a two-step motion following the Lipari-Szabo model.[42,43] According to the model, in the first step, the correlation function decays from unity to a value referred to as an order parameter, S, which reflects incomplete averaging of the spin (in this case, dipole-dipole) interactions due to a restricted (anisotropic) motion. Then, in the second step, the correlation function decays from S to zero due to a slower dynamics. The faster process, characterized by the correlation time $\tau_{c,2}$ and the dipolar relaxation constant $C_{DD,2}^{HH}$, is responsible for the first step of the decay of the correlation function. As with increasing temperature, the motion becomes less anisotropic (restricted) the order parameter, S, becomes smaller (for fully isotropic motion, one gets $S = 0$). In consequence, the dipolar relaxation constant for the slower process, $C_{DD,1}^{HH} = S\, C_{DD,2}^{HH}$, decreases with increasing temperature. The concept that the fast process becomes more isotropic is supported by the increase of the relaxation constant $C_{DD,2}^{HH}$ with temperature, from 9.7×10^7 Hz^2 at 236 K to 1.6×10^8 Hz^2 at 276 K and above. One could expect a progressive increase of $C_{DD,2}^{HH}$ with temperature (it becomes constant above 273 K), but this is a matter of the accuracy of the fit limited by the presence of some relaxation enhancement effects around 10 MHz (we shall comment on that later) and the fact that at high temperatures $C_{DD,2}^{HH}$ is almost one order of magnitude smaller than $C_{DD,1}^{HH}$.

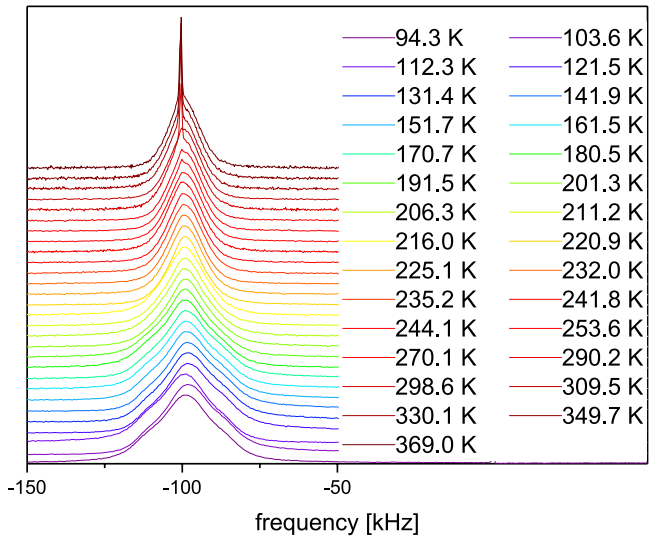

FIG. 5. ^{1}H NMR spectra for $[C_3H_5N_2]_6[Bi_4Br_{18}]$ collected at 91 MHz. "Off resonance" FID spectra have been recorded as indicated by the frequency scale.

The ^{1}H spectra shown in Fig. 5 confirm that the faster motional process is anisotropic. The linewidth (full width at half maximum - FWHM) varies from about 22 kHz at 94 K down to about 11.5 kHz at 369 K. During some runs (at 299 K, 330 K, 350 K, and 369 K), some liquid water outside the sample was left. Therefore, the spectra at the highest temperatures contain water peaks. Even at the highest temperatures, the spectra are much broader than the water peaks thereby indicating the anisotropy of the faster dynamical process.

The shape of the QRE maxima show that the slower process cannot become significantly faster with increasing temperature, because then the QRE peaks would become broader and less pronounced, in contrary to the experimental finding. It is worth to mention that dielectric spectroscopy studies of $[C_3H_5N_2]_6[Bi_4Br_{18}]$ also show two motional processes and the amplitude of the faster process is considerably larger ($\Delta\varepsilon \approx$ 8-9) than of the slower one ($\Delta\varepsilon \approx 0.5$).[37]

The QRE pattern has given direct access to the ^{14}N quadrupole parameters. At this stage, two features of the R_1 relaxation dispersion profiles should be pointed out. The first one is that in the low frequency range of about 30 kHz-100 kHz, one sees additional QRE peaks (for instance, Fig. 4(b)). We have omitted this effect in the analysis, but the presence of the additional relaxation maxima indicates that there is a fraction of ^{14}N nuclei in $[C_3H_5N_2]_6[Bi_4Br_{18}]$ which experience a considerably smaller electric field gradient at their position. This observation is a demonstration of the sensitivity of ^{1}H FC NMR relaxometry to structural properties of the investigated compounds. Moreover one also observes some QRE effects at high frequencies, around 10 MHz (for 296 K and below–Figs. 4(a) and 4(b)) which we have neglected in the analysis. They stem from ^{1}H-^{35}Br QRE; one can also expect some effects at even higher frequencies (beyond the accessible frequency range) associated with ^{1}H-^{83}Bi interactions. Actually at almost all temperatures, the experimental step width, which was chosen to be constant on a logarithmic scale, was too broad to allow for probing the peaks in detail. Only at 236 K, the step was decreased. And, indeed, the existence of

the peaks was confirmed. Finishing this discussion, we again stress that although we have included into the analysis the very low frequency range trying to well reproduce the experimental data, around 25 kHz, we are approaching the situation when the ^{1}H-^{1}H dipole-dipole coupling is no longer much smaller than the ^{1}H Zeeman interaction (Fig. 5) which might somewhat affect the theoretical predictions based on the perturbation theory (which assumes that the dipolar Hamiltonian is a small perturbation).

V. CONCLUSIONS

We have employed ^{1}H NMR FC relaxometry to inquire dynamical features of the compound $[C_3H_5N_2]_6[Bi_4Br_{18}]$ which shows a rich polymorphism in the solid state. The investigations have been carried out in the temperature range 236 K-382 K which corresponds to phase II of the compound. It has been shown that the overall ^{1}H spin-lattice relaxation dispersion profiles can be decomposed into three contributions corresponding to a ^{1}H-^{1}H relaxation pathway modulated by a slow motional process, a ^{1}H-^{14}N contribution also modulated by the slow dynamics giving rise to QRE effects, and a sum of ^{1}H-^{1}H and ^{1}H-^{14}N relaxation contributions associated with a faster motional process. These two terms are hardly distinguishable. The two motional processes can be considered as a "two-step" dynamics of imidazolium cations. The faster motion is characterized by the dipolar relaxation constant $C_{DD,2}^{HH} = 1.6 \times 10^8$ Hz^2 (reduced at the lowest temperatures, 256 K and 236 K) and a correlation time ranging from $\tau_{c,2} \cong 1.5 \times 10^{-7}$ s at 236 K down to $\tau_{c,2} \cong 6 \times 10^{-9}$ s at 382 K. The dipolar relaxation constant of the slower motional process decreases with increasing temperature from $C_{DD,1}^{HH} = 1.1 \times 10^8$ Hz^2 to 2×10^7 Hz^2, while the correlation time appears to be hardly temperature dependent ($\tau_{c,1} = 1.2 \times 10^{-5}$ s). One should stress at this stage that one could assume a weak dependence of $\tau_{c,1}$ on temperature and compensate the effect by the corresponding relaxation constant, but we decided against that as the conclusion would remain unchanged. This correlation time allows for reproducing the shape of the QRE maxima leading to an acceptable agreement with the experimental data in the whole temperature range. The quadrupolar parameters, a_Q and η, show a temperature dependence, which is reflected in the positions of the relaxation peaks. The QRE pattern has been described using a general theory valid for arbitrary motional conditions and interaction strengths (i.e., not restricted to the conditions required by perturbation theories of relaxation) and is applied, to our knowledge, for the first time to such a large data set. The reported ^{1}H spin-lattice relaxation data and their rather involved analysis give access to dynamical and structural features (the electric field gradient determining the position of the relaxation peaks reflects subtle changes in the molecular arrangement) of the crystal, illustrating the potential of NMR relaxometry.

Uncertainty of $C_{DD,2}^{HH}$ and $\tau_{c,2}$ does not exceed 10%, for $\tau_{c,1}$, at 382 K it yields about 20% (at lower temperatures, this parameter has been kept constant); uncertainty of $C_{DD,1}^{HH}$ ranges between 15% and 30% (for lower temperatures when the low frequency peaks neglected in the analysis are present).

ACKNOWLEDGMENTS

This research was supported by National Science Centre, Poland, Grant No. DEC-2012/05/B/ST3/03190.

[1]R. Kimmich and N. Fatkullin, Adv. Polym. Sci. **170**, 1 (2004).
[2]J. P. Korb and R. G. Bryant, Adv. Inorg. Chem. **57**, 293 (2005).
[3]D. Kruk, A. Herrmann, and E. A. Rössler, Prog. Nucl. Magn. Reson. Spectrosc. **63**, 33 (2012).
[4]F. Noack, Prog. Nucl. Magn. Reson. Spectrosc. **18**, 171 (1986).
[5]O. Lips, D. Kruk, A. F. Privalov, and F. Fujara, Solid State Nucl. Magn. Reson. **31**, 141 (2007).
[6]D. Kruk, A. Privalov, W. Medycki, C. Uniszkiewicz, W. Masierak, and R. Jakubas, Annu. Rep. NMR Spectrosc. **76**, 67 (2012).
[7]I. Solomon and N. Bloemebergen, J. Chem. Phys. **25**, 261 (1956).
[8]A. Abragam, *The Principles of Nuclear Magnetism* (Oxford University Press, Oxford, 1961).
[9]C. Slichter, *Principles of Magnetic Resonance* (Springer-Verlag, Berlin, 1990).
[10]D. Kruk, R. Meier, and E. A. Rossler, J. Phys. Chem. B **115**, 951 (2011).
[11]D. Kruk, R. Meier, and E. A. Rossler, Phys. Rev. E **85**, 020201 (2012).
[12]N. Bloembergen and L. O. Morgan, J. Chem. Phys. **34**, 842 (1961).
[13]D. Kruk, A. Kubica, W. Masierak, A. F. Privalov, M. Wojciechowski, and W. Medycki, Solid State Nucl. Magn. Reson. **40**, 114 (2011).
[14]F. Winter and R. Kimmich, Biochim. Biophys. Acta **719**(2), 292 (1982).
[15]M. Nolte, A. Privalov, J. Altmann, V. Anferov, and F. Fujara, J. Phys. D: Appl. Phys. **35**, 939 (2002).
[16]D. Kruk, J. Altmann, F. Fujara, A. Gadke, M. Nolte, and A. F. Privalov, J. Phys.: Condens. Matter **17**(3), 519 (2005).
[17]D. J. Schneider and J. H. Freed, Adv. Chem. Phys. **73**, 387 (1989).
[18]Z. Liang and J. H. Freed, J. Phys. Chem. B **103**, 6384 (1999).
[19]T. Nilsson and J. Kowalewski, J. Magn. Reson. **146**, 345 (2000).
[20]D. Kruk, *Theory of Evolution and Relaxation of Multi-Spin Systems. Application to Nuclear Magnetic Resonance (NMR) and Electron Spin Resonance (ESR)* (Abramis Academic, Arima Publishing, UK, 2007).
[21]D. Kruk, J. Kowalewski, S. Tipikin, J. H. Freed, M. Mościcki, A. Mielczarek, and M. Port, J. Chem. Phys. **134**(2), 024508 (2011).
[22]E. Belorizky, P. H. Fries, L. Helm, J. Kowalewski, D. Kruk, R. R. Sharp, and P.-O. Westlund, J. Chem. Phys. **128**, 052315 (2008).
[23]K. Åman and P.-O. Westlund, Phys. Chem. Chem. Phys. **9**, 691 (2007).
[24]P.-O. Westlund, Mol. Phys. **107**, 2141 (2009).
[25]P.-O. Westlund, Phys. Chem. Chem. Phys. **12**, 3136 (2010).
[26]N. F. Peirson, J. A. S. Smith, and D. Stephenson, Z. Naturforsch. **49**, 345 (1994).
[27]Y. L. Wang and P. S. Belton, Chem. Phys. Lett. **325**, 33 (2000).
[28]J. A. S. Smith, T. J. Rayner, M. D. Rowe, J. Barras, N. F. Peirson, A. D. Stevens, and K. Althoeferm, J. Magn. Reson. **204**, 139 (2010).
[29]E. P. Sunde and B. Halle, J. Magn. Reson. **203**, 257 (2010).
[30]D. J. Lurie, G. R. Davies, M. A. Foster, and J. M. S. Hutchison, Magn. Reson. Imaging **23**, 175 (2005).
[31]R. Jakubas, Z. Ciunik, and G. Bator, Phys. Rev. B **67**, 024103 (2003).
[32]A. Piecha, A. Białońska, and R. Jakubas, J. Mater. Chem. **22**, 333 (2012).
[33]W. Bi, N. Leblanc, N. Mercier, P. Auban-Senzier, and C. Pasquier, Chem. Mater. **21**, 4099 (2009).
[34]A. Piecha, A. Białońska, and R. Jakubas, J. Phys.: Condens. Matter **20**, 325224 (2008).
[35]R. Jakubas, A. Piecha, A. Pietraszko, and G. Bator, Phys. Rev. B **72**, 104107 (2005).
[36]J. Zaleski, Cz. Pawlaczyk, R. Jakubas, and H. G. Unruh, J. Phys.: Condens. Matter **12**, 7509 (2000).
[37]A. Piecha, R. Jakubas, A. Pietraszko, J. Baran, W. Medycki, and D. Kruk, J. Solid State Chem. **182**, 2949 (2009).
[38]A. G. Redfield, in *Encyclopedia of Nuclear Magnetic Resonance*, edited by D. M. Grant and R. K. Harris (Wiley, Chichester, 1996), p. 4085.
[39]D. A. Varshalovich, A. N. Moskalev, and V. K. Khersonkii, *Quantum Theory of Angular Momentum* (World Scientific Publishing, Singapore, 1988).
[40]F. Fujara, D. Kruk, and A. Privalov, Prog. Nucl. Magn. Reson. Spectrosc. **82**, 39 (2014).
[41]B. Kresse, A. F. Privalov, and F. Fujara, Solid State Nucl. Magn. Reson. **40**, 134 (2011).
[42]G. Lipari and A. Szabo, J. Am. Chem. Soc. **104**, 4546 (1982).
[43]J. Kowalewski and L. Mäler, *Nuclear Spin Relaxation in Liquids: Theory, Experiments, and Applications* (Taylor & Francis, New York, 2006).